

# Homo- and heteromeric interaction strengths of the synergistic antimicrobial peptides PGLa and magainin 2 in membranes

Jonathan Zerweck<sup>1</sup> · Erik Strandberg<sup>2</sup> · Jochen Bürck<sup>2</sup> · Johannes Reichert<sup>2</sup> · Parvesh Wadhvani<sup>2</sup> · Olga Kukharensko<sup>1</sup> · Anne S. Ulrich<sup>1,2</sup>

Received: 16 December 2015 / Revised: 1 February 2016 / Accepted: 16 February 2016 / Published online: 6 April 2016  
© European Biophysical Societies' Association 2016

**Abstract** PGLa and magainin 2 (MAG2) are amphiphilic  $\alpha$ -helical frog peptides with synergistic antimicrobial activity. In vesicle leakage assays we observed the strongest synergy for equimolar mixtures of PGLa and MAG2. This result was consistent with solid-state <sup>15</sup>N-NMR data on the helix alignment in model membranes. The Hill coefficients determined from the vesicle leakage data showed that the heterodimeric (PGLa-MAG2) interactions were stronger than the homodimeric (PGLa-PGLa and MAG2-MAG2) interactions. This result was also reflected in the free energy of dimerization determined from oriented circular dichroism and quantitative solid-state <sup>19</sup>F-NMR analysis.

**Keywords** Synergistic antimicrobial peptides · Membrane-active amphiphilic helices · Solid-state NMR · Vesicle leakage assay · Hill coefficients · Peptide dimerization

## Introduction

Antimicrobial peptides (AMPs) are found in almost all types of organisms, including bacteria, plants, and mammals, and they form an important part of the defence

against intruding microorganisms (Boman 1991, 2003; Brogden 2005; Pinheiro da Silva and Machado 2012). There is increasing interest in AMPs and in understanding their mechanism of action. Particularly intriguing is the synergy observed between certain AMPs. A well-studied example is the synergistic pair PGLa (GMASK-AGAIAGKIAKVALKAL-NH<sub>2</sub>) and magainin 2 (MAG2) (GIGKFLHSAKKFGKAFVGEIMNS-OH), both found in the skin of the African frog *Xenopus laevis* (Soravia et al. 1988; Strandberg et al. 2009; Zasloff 1987). Both peptides are unstructured in aqueous solution but form amphipathic  $\alpha$ -helices in the presence of membranes, as shown by circular dichroism (Glaser et al. 2004; Latal et al. 1997; Matsuzaki et al. 1991). Helical wheel projections are shown in Fig. 1. Both peptides have one main hydrophobic face and one polar (charged) face, the polar sector of PGLa (approximately 120°) being significantly smaller than that of MAG2 (approximately 180°).

Synergistic activity between PGLa and MAG2 has been demonstrated in several biophysical and biological assays, including membrane potential dissipation (Juretic 1990), release of carboxyfluorescein from liposomes (Williams et al. 1990), membrane permeabilization (Vaz Gomes et al. 1993), liposome permeabilization, antimicrobial activity, and toxic effects on tumor cells (Westerhoff et al. 1995). Furthermore, several mutants of PGLa and MAG2 have also shown synergistic antimicrobial activity (Glattard et al. 2016; Matsuzaki et al. 1998; Strandberg et al. 2015) in studies aiming to characterize the synergistic assembly of the two peptides. It seems likely that all of these synergistic effects are due to the same underlying assembly of the two peptides, which enhances their ability to permeabilize membranes; however, the mechanism behind this is not well understood.

It has been reported that mixtures of PGLa and MAG2 elicit the maximum membrane permeabilization at a 1/1

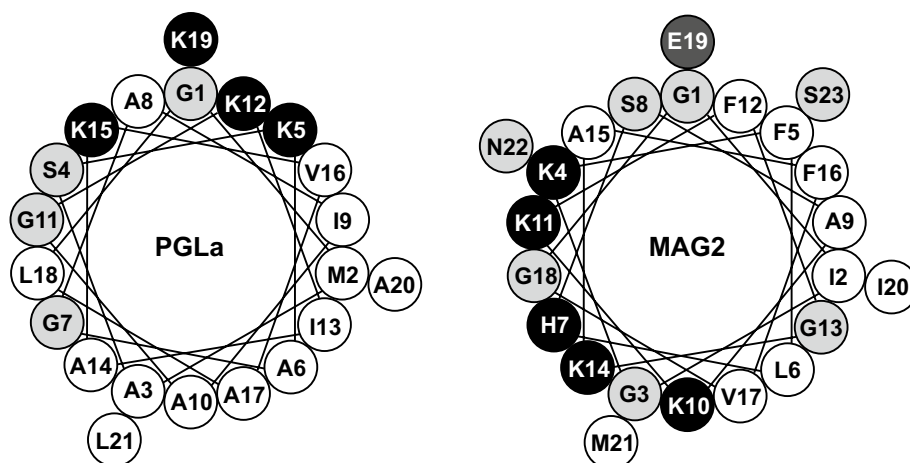
**Electronic supplementary material** The online version of this article (doi:10.1007/s00249-016-1120-7) contains supplementary material, which is available to authorized users.

✉ Anne S. Ulrich  
anne.ulrich@kit.edu

<sup>1</sup> Karlsruhe Institute of Technology (KIT), Institute of Organic Chemistry, Fritz-Haber-Weg 6, 76131 Karlsruhe, Germany

<sup>2</sup> KIT, Institute of Biological Interfaces (IBG-2), POB 3640, 76021 Karlsruhe, Germany

**Fig. 1** Helical wheels of PGLa and MAG2. The amino acids are color-coded: hydrophobic residues are white, cationic residues are black, anionic residues are dark grey, polar residues and Gly are light grey



molar ratio, which indicates that the two peptides may form a 1/1 complex in the membrane, presumably as a heterodimer (Matsuzaki et al. 1998). Several studies have shown that MAG2 and related peptides can form dimers (Gesell et al. 1997; Matsuzaki et al. 1998, 1994; Porcelli et al. 2006; Wakamatsu et al. 2002), and the same holds for PGLa (Glaser et al. 2005; Strandberg et al. 2006; Tremouilhac et al. 2006a; Wang et al. 2014). Dimerization seems to be essential for the synergistic activity, because disulphide-linked MAG2 dimers show higher permeabilization and antimicrobial activity than the monomeric peptides (Dempsey et al. 2003; Hara et al. 2001a). Cross-linking experiments have indicated that PGLa and MAG2 tend to form parallel heterodimers in PC/PG membranes but not in solution. The cross-linked parallel heterodimers show a much higher membrane permeabilization activity than that of the individual peptides alone, indicating that the observed synergism can indeed be explained by the formation of heterodimeric assemblies (Hara et al. 2001b).

The orientation of the two peptides in membranes has been thoroughly studied using solid-state NMR, a method of choice to determine helix orientations in lipid bilayers (Strandberg and Ulrich 2004; 2014; Ulrich 2005; Ulrich et al. 2006; Wadhvani et al. 2007). PGLa re-orientates in the presence of MAG2, which appears to be related to the synergistic effects. On its own, MAG2 has been found to lie rather flat on the membrane, in a so-called surface state (“S-state”) (Strandberg et al. 2013), whereas PGLa is in an S-state at low concentrations but re-orientates to a more tilted “T-state” at higher concentrations (Glaser et al. 2005; Strandberg et al. 2006; Tremouilhac et al. 2006a). When the two peptides are mixed in a 1/1 molar ratio, PGLa changes its orientation to a transmembrane inserted state (“I-state”) (Salnikov and Bechinger 2011; Strandberg et al. 2013; Tremouilhac et al. 2006b), and MAG2 also slightly changes its orientation to a T-state (Strandberg et al. 2013). The inserted orientation of PGLa would be compatible with

the formation of stable water-filled transmembrane pores lined by PGLa, while MAG2 stays on the membrane surface and is needed to stabilize the pore (Strandberg et al. 2013). This model may explain the synergistic activity of the two peptides.

In the present study, we set out to investigate the assembly of PGLa and MAG2 in model membranes and to quantitatively examine the formation of the presumed heterodimers. Only little is known about the interaction strength, which was studied here with a fluorescence-based vesicle leakage assay, giving a Hill coefficient that describes the cooperativity of the peptides. We also investigated the concentration dependence of the interaction using the exceptional sensitivity of  $^{19}\text{F}$ -NMR, which makes it possible to study peptides in membranes at a peptide-to-lipid molar ratio (P/L) as low as 1/3000 (Glaser and Ulrich 2003; Wadhvani et al. 2012, 2014, 2008). From these data and previous oriented circular dichroism studies (Bürck et al. 2008; Ludtke et al. 1994), we estimated the free energy of dimerization of the two peptides in the membrane and found that heterodimers are more likely to form than homodimers of either peptide.

## Materials and methods

### Materials

Fmoc-protected amino acids and reagents for peptide synthesis were purchased from Iris Biotech GmbH (Marktredwitz, Germany) or Novabiochem (Merck Chemicals Ltd., Nottingham, UK). The  $^{19}\text{F}$ -labeled amino acid *L*-3- $\text{CF}_3$ -bicyclopent-[1.1.1]-1-yl-glycine ( $\text{CF}_3$ -Bpg) was obtained from Enamine (Kiev, Ukraine). The  $^{15}\text{N}$ -labeled Ala was purchased from Cambridge Isotope Laboratories (Andover, MA, USA) and was Fmoc-protected using Fmoc-Cl, as previously described (Carpino

and Han 1972). All solvents required for synthesis and HPLC purification were from Acros Organics (Geel, Belgium) or Biosolve (Valkenswaard, The Netherlands). The UV-grade chloroform and methanol used for NMR sample preparation were from VWR International (Bruchsal, Germany). The lipids 1,2-dimyristoyl-*sn*-glycero-3-phosphatidylcholine (DMPC), 1,2-dimyristoyl-*sn*-glycero-3-phosphatidylglycerol (DMPG), 1-palmitoyl-2-oleoyl-*sn*-glycero-3-phosphatidylcholine (POPC), 1-palmitoyl-2-oleoyl-*sn*-glycero-3-phosphatidylglycerol (POPG), 1',3'-bis[1,2-dioleoyl-*sn*-glycero-3-phospho]-*sn*-glycerol (TOCL), and 1,2-dioleoyl-*sn*-glycero-3-phosphoethanolamine-*N*-(lissamine rhodamine B sulfonyl) (Rhod-PE) were obtained from Avanti Polar Lipids (Alabaster, AL, USA) or NOF Europe (Grobendonk, Belgium). ANTS and DPX were from Invitrogen (Eugene, OR, USA). Triton-X-100, HEPES, and Sephadryl 100-HR were from Sigma-Aldrich Chemie GmbH (Steinheim, Germany).

### Peptide synthesis

PGLa, with the sequence GMASKAGAIAGKIAKVAL-KAL-NH<sub>2</sub>, was synthesized with <sup>15</sup>N-Ala at position 10 at a 100 μmol scale on an automated Syro II peptide synthesizer (MultiSynTech, Witten, Germany). The <sup>15</sup>N-Ala was coupled manually in DMF by using Fmoc-<sup>15</sup>N-Ala in the presence of 1-hydroxybenzotriazole (HOBt), 1-benzotriazole-1-yl-*N,N,N',N'*-tetramethyluronium hexafluorophosphate (HBTU) and *N,N*-diisopropylethylamine (DIPEA) as a base in a molar ratio of 2/2/2/4, respectively. Magainin 2 (MAG2), with the sequence GIGKFLHSAKKFGKAF-VGEIMNS-OH, was synthesized on an automated Liberty 1 microwave peptide synthesizer (CEM, Kamp-Lintfort, Germany) at a 250-μmol scale. The peptides were purified via HPLC using C18 reverse phase HPLC columns with water/acetonitrile gradients, each containing 5 mM HCl as the ion pair agent. The purity of the peptides was confirmed using an LC-MS system equipped with an Agilent 1100 Series LC-system coupled to an ESI μ-TOF mass spectrometer from Bruker Daltonics.

### Vesicle leakage assay

#### Vesicle preparation

The appropriate lipids for each experiment were dissolved in CHCl<sub>3</sub>, together with 0.02 mol% Rhod-PE. The solvent was removed, and the dried lipids were hydrated in 10 mM HEPES buffer (pH 7.5) containing 12.5 mM ANTS, 45 mM DPX, and 50 mM NaCl. This stock suspension was subjected to ten freeze–thaw cycles and then frozen. Appropriate aliquots of the stock lipid suspension were thawed each day and extruded (41 times) through

polycarbonate membranes with a 100-nm pore size and stored at room temperature overnight. The fluorophore and quencher that were not contained within the vesicles were removed by size-exclusion chromatography using spin-columns (Pierce centrifuge column, 2 ml, Life Technologies GmbH, Darmstadt, Germany) filled with Sephadryl 100-HR (2 min, 1500 × *g*). A 10 mM HEPES buffer (pH 7.5) containing 155 mM NaCl to balance the osmolarity was used for elution. After extrusion and the removal of the external dye and quencher, the lipid concentration usually decreases. Therefore, before each set of measurements, a rhodamine spectrum was recorded to determine the actual concentration of lipids, which was referenced to a spectrum of vesicles prepared by sonification without any subsequent treatment.

#### Measurements

Fluorescence measurements were performed on a FluoroMax2 spectrofluorometer (HORIBA Jobin–Yvon, Unterhaching, Germany) equipped with a thermostated sample holder and magnetic stirrer using an excitation wavelength of 355 nm, an emission wavelength of 508 nm, and slit widths of 5 nm. The peptide solutions were placed in elution buffer in a 1-cm standard cuvette. One hundred seconds after the start of the measurement, the lipid vesicles were added, and the intensity of the fluorescence at 508 nm was recorded. The leakage was measured for 180 or 600 s after the addition of the vesicles, and the measurement was terminated after addition of Triton-X-100 (0.25 % v/v), which dissolved the vesicles, and yielded 100 % leakage. To determine the background signal of the vesicles themselves, several blanks were recorded in each set of measurements. In this assay, leakage is observed when the pores are large enough to allow the dye molecules to pass (molecular weights of ANTS and DPX is 381 and 262 Da, respectively), which can be estimated to be around 10 Å (Rex 1996).

We defined a synergy factor SF, to be calculated from the leakage values of PGLa, MAG2, and of the mixture of these two peptides:

$$SF = \frac{L(P + M)}{L(P) + L(M)} \quad (1)$$

Here,  $L(P)$  is the leakage observed with PGLa alone,  $L(M)$  is the leakage observed with MAG2 alone, and  $L(P+M)$  is the leakage observed with the mixture. In all cases, the total  $P/L$  was kept constant. Because the leakage was very sensitive to small changes in the peptide and lipid concentration, the  $P/L$  was slightly adjusted each day to obtain the same amount of leakage for the 1:1 mixture, which was the internal standard used to guarantee comparable conditions each measurement day.

### Hill coefficients

The results of leakage experiments were analyzed according to the Hill equation (Endrenyi et al. 1975; Steinbrecher et al. 2012):

$$v(c) = v_{\max} \times \frac{c^n}{K_H^n + c^n} \quad (2)$$

where  $v_{\max}$  is the maximal leakage rate (in %/s),  $c$  is the peptide concentration (in  $\mu\text{M}$ ),  $K_H$  is the half-maximal activity constant (representing the peptide concentration [in  $\mu\text{M}$ ] at which the half-maximal rate is reached), and  $n$  is the Hill coefficient.

### Solid-state NMR

#### NMR sample preparation

Usually, 0.5–0.6 mg of the  $^{15}\text{N}$ -labeled peptide was used, along with appropriate amounts of the synergistic peptide and lipids to obtain the desired  $P/L$  ratio of 1/50. Typically, 0.1–0.3 mg of  $^{19}\text{F}$ -labeled peptide was used in the samples for  $^{19}\text{F}$ -NMR. We used DMPC/DMPG (3/1) as the lipid system. PGLa/MAG2 ( $^{15}\text{N}/^{19}\text{F}$ ) was suspended in MeOH (40  $\mu\text{l}$ ) and solubilized by adding water (20  $\mu\text{l}$ ). In samples with two peptides, both peptides were separately dissolved in water (10  $\mu\text{l}$ ). MeOH (40  $\mu\text{l}$ ) was added to the solution containing the unlabeled peptide, and this was transferred to the labeled peptide solution. The lipids were dissolved in 120  $\mu\text{l}$  of chloroform and 160  $\mu\text{l}$  of methanol, and the lipid solution was added to the peptide solution. The lipid vessel was rinsed with additional chloroform (50  $\mu\text{l}$ ), which was also added to the peptide solution. The final container was always the one containing the labeled peptide. After 5 min of sonification, the resulting clear solution was uniformly spread onto 23 glass plates with dimensions of 7.5 mm  $\times$  9 mm  $\times$  0.08 mm (Marienfeld Laboratory Glassware, Lauda-Königshofen, Germany). After the organic solvent was evaporated under reduced pressure, the glass plates were stacked and hydrated for 16–24 h at 48 °C in a humidity chamber with a saturated solution of  $\text{K}_2\text{SO}_4$ , producing 96 % relative humidity in the chamber (Greenspan 1977). To keep the sample fully hydrated throughout the measurements, it was wrapped in parafilm and polyethylene foil. The sample quality was determined by monitoring the degree of lipid orientation using solid-state  $^{31}\text{P}$ -NMR.

#### NMR experimental details

$^1\text{H}$ - $^{15}\text{N}$  cross-polarization experiments using a CP-MOIST pulse sequence (Levitt et al. 1986) were performed on an Avance III Bruker NMR spectrometer (Bruker Biospin, Karlsruhe, Germany) with a wide bore 500- or 600-MHz

resonance frequency magnet. The spectra were acquired using a double-tuned probe with a low-E flat-coil resonator (3 mm  $\times$  9 mm cross section) and typically used a  $^1\text{H}$  and  $^{15}\text{N}$  radiofrequency field strength of 65 kHz during the cross-polarization and 36 kHz  $^1\text{H}$  SPINAL16 decoupling (Fung et al. 2000) during acquisition. Approximately 10,000–30,000 scans were accumulated with mixing times of 500 or 1000  $\mu\text{s}$ . The acquisition time was 10 ms, and the recycle time was 3 s. The  $^{15}\text{N}$  chemical shift was referenced using an ammonium sulphate dry powder sample, and the  $^{15}\text{N}$  chemical shift was set to 26.8 ppm.

The  $^{19}\text{F}$ -NMR experiments were performed on a home-built flat-coil  $^{19}\text{F}/^1\text{H}$  probe head using an anti-ringing sequence to reduce the background signals from the probe (Zhang et al. 1990), with a 2.3- $\mu\text{s}$  90° pulse, a 1-s relaxation delay time, a 500-kHz spectral width, 4096 data points, and proton decoupling with a tpm20 sequence (Bennett et al. 1995). Between 20,000 and 80,000 scans were typically collected. After zero filling to 16,384 data points and an exponential multiplication of 200–1000 Hz, a Fourier transformation was performed. The spectra were referenced to a 100 mM NaF solution for which the  $^{19}\text{F}$  signal was set to  $-119.5$  ppm.

To determine the sample quality (hydration and degree of lipid orientation),  $^{31}\text{P}$ -NMR measurements were performed using a Hahn echo sequence (Rance and Byrd 1983), with a typical 90° pulse of 3.9  $\mu\text{s}$ , a 35  $\mu\text{s}$  echo time, and  $^1\text{H}$  SPINAL64 decoupling during acquisition. Typically, 256 scans were accumulated. The acquisition time was 10 ms, and the recycle time was 1 s. All NMR measurements were obtained at 35 °C. The temperature of the sample inside the NMR probe was calibrated using a methanol sample (Ammann et al. 1982).

### Free energy calculations

The association constant  $K$  that describes the monomer-dimer equilibrium in the membrane depends only on the peptide/lipid ratio (Chen et al. 2009; You et al. 2005) and is given by:

$$K = \frac{[D]}{[M]^2} \quad (3)$$

where  $[D]$  is the molar concentration of the dimer in the membrane (dimers per lipid) and  $[M]$  is the molar concentration of the monomer in the membrane (monomers per lipid). The free energy of dimerization is calculated as:

$$\Delta G_d = -RT \ln K \quad (4)$$

For the formation of heterodimers from PGLa and MAG2, the equilibrium constant is changed slightly. A more complex analysis can be found in (Matsuzaki et al. 1998), but we will assume that the heterodimers are formed

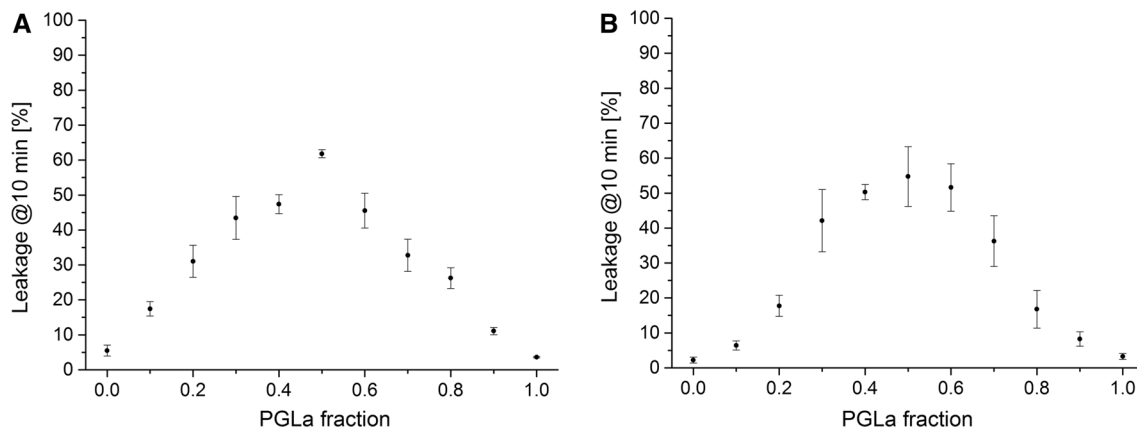


**Fig. 2** Job-plots of vesicle leakage as a function of the molar fraction of PGLa in mixtures of PGLa and MAG2. The leakage values were measured 600 s after adding the peptides to the vesicle suspension. In POPC/POPG (3/1 molar ratio), the total *P/L* ratio was always 1/160, whereas in POPE/POPG/TOCL (72/23/5), the total *P/L* was 1/35. The

lipid concentration was 100  $\mu$ M, and the temperature was 30  $^{\circ}$ C. The data presented here are averages of three series of measurements. **a** Vesicles of POPC/POPG (3/1). **b** Vesicles of POPE/POPG/TOCL (72/23/5)

with a much higher affinity than the homodimers (see values below and in (Matsuzaki et al. 1998)). We can then disregard homodimer formation and have the equilibrium reaction



where *P* is PGLa, *M* is MAG2, and *PM* is the PGLa/MAG2 heterodimers. We then obtain the equilibrium constant:

$$K = \frac{[PM]}{[P][M]} \quad (6)$$

where [*P*] is the molar concentration of the PGLa monomer in the membrane (monomer per lipid), [*M*] is the corresponding concentration of the MAG2 monomer, and [*PM*] is the molar concentration of the heterodimer (dimer per lipid). By starting with an equimolar mixture of PGLa and MAG2, [*P*] = [*M*], the heterodimer formation will not change this equilibrium. We can then use Eq. (4) to calculate  $\Delta G_d$  for the heterodimer formation.

## Results and discussion

### Determination of the molar ratio for maximal synergy

The synergy of PGLa and MAG2 can be studied using several different methods. Previously, it has been shown through MIC assays and checkerboard assays that the two peptides possess highly synergistic antimicrobial activity (Matsuzaki et al. 1998; Ruden et al. 2009; Strandberg et al. 2015; Westerhoff et al. 1995). Here, we used vesicle leakage assays and solid state NMR, and from these complementary methods, we attempted to obtain more detailed

insights to understand the synergy. In all experiments, we use lipids in the biologically relevant liquid crystalline phase.

In the literature, it has been reported that the maximum synergy for PGLa and MAG2 in a leakage assay is elicited at a 1/1 molar ratio (Matsuzaki et al. 1998). To test whether this could be reproduced in our experiments, we measured leakage at different PGLa/MAG2 molar ratios in two types of lipid vesicles. Many different lipid compositions have been used in the past for vesicle leakage assays to study, e.g., the effect of acyl chain length, lipid charge, or cholesterol on leakage (Lee et al. 2013; Cujova et al. 2014; Grau-Campistany et al. 2015). Here, we keep those factors constant but vary the lipid spontaneous curvature. A POPC/POPG (3/1) mixture is often used in model membranes, while POPE/POPG/TOCL (72/23/5) has been used to specifically mimic bacterial membranes, because this mixture is similar to the lipid composition of *E. coli* membranes (Avanti Polar Lipids 2015; Raetz 1978). Figure 2a presents the job-plots for the POPC/POPG vesicles, and Fig. 2b presents the job-plots for the POPE/POPG/TOCL vesicles. In both cases, the maximum leakage was found at a 1/1 molar ratio of the two peptides, confirming the literature results. The synergy factor was determined for the 1/1 peptide mixture. In POPC/POPG the mixture indeed showed  $11.4 \pm 3.1$  times-higher leakage compared to the sum of the activities of the single peptides at the same total peptide concentration. In POPE/POPG/TOCL, the synergy factor was  $18.0 \pm 5.9$ .

When comparing the synergy factors in the two different lipid systems, we note that a different total *P/L* ratio was used for the two series of measurements. That is because the peptide concentration had to be chosen such that the

full dynamic range was utilized (i.e., neither should the maximum leakage exceed 100 %, nor should the smallest signals be too weak). The total *P/L* ratio was always 1/160 in POPC/POPG (3/1), whereas in POPE/POPG/TOCL (72/23/5) the total *P/L* was 1/35. In both cases, the 1/1 peptide mixture gave around 60 % leakage, so it was obviously easier to induce leakage in the POPC/POPG system than in the more realistic bacterial membrane model. This finding was expected, since it has been shown that amphiphilic peptides can more easily insert into membranes with a more positive spontaneous curvature (Strandberg et al. 2012, 2013; Strandberg and Ulrich 2015). POPE and TOCL, however, are lipids with small headgroups and therefore have strongly negative spontaneous curvatures. Despite their different susceptibilities towards peptide-induced leakage, it was remarkable to find that the synergy factor in the lipid mixture that mimicked the bacterial membrane was about twice as large as that in the simpler lipid system. This observation suggests that the synergistic peptide interaction may be optimized to bacterial membranes.

The alignment angle of a helical peptide relative to the bilayer normal can be estimated from the chemical shift of the  $^{15}\text{N}$ -labeled backbone, when the peptide is reconstituted in macroscopically oriented lipid membranes (Bechinger et al. 1996; Glaser et al. 2005; Grage et al. 2012; Strandberg and Ulrich 2004; Strandberg et al. 2013; Walther et al. 2010). Here, synergy between the peptides was monitored in DMPC/DMPG (3/1) bilayers by observing the concomitant re-orientation of  $^{15}\text{N}$ -labeled PGLa. PGLa alone yielded a signal with a chemical shift of 133 ppm, corresponding to an obliquely tilted helix (T-state) in the membrane (Fig. 3a). From earlier  $^{19}\text{F}$ - and  $^2\text{H}$ -NMR studies, the tilt angle of PGLa in DMPC/DMPG at *P/L* = 1/50 is known to be close to  $125^\circ$  (Glaser et al. 2005; Strandberg et al. 2006; Tremouilhac et al. 2006a). In a 1/1 mixture with MAG2, PGLa yielded a signal at 205 ppm (Fig. 3c), which corresponds to a fully inserted peptide (I-state) with a tilt of approximately  $20^\circ$  (Salnikov and Bechinger 2011; Strandberg et al. 2009, 2013; Tremouilhac et al. 2006b). If a 1/1 complex of the two peptides were to be responsible for the inserted state, then we would assume that in a peptide mixture with less MAG2 than PGLa, only part of the PGLa peptides would be inserted. Indeed, two  $^{15}\text{N}$ -NMR peaks became visible when a 2/1 mixture of PGLa/MAG2 was studied. The spectrum (Fig. 3b) shows a main peak at 186 ppm, corresponding to inserted PGLa (in complex with MAG2), and another signal at 95 ppm, which corresponds to PGLa (not in complex with MAG2) lying flat on the membrane surface (S-state). Because two distinct signals were present, there was no fast exchange between the two states on the NMR time scale. This finding leads to the conclusion that there are distinct populations of peptides, and that the interaction between the synergistic pairs represents

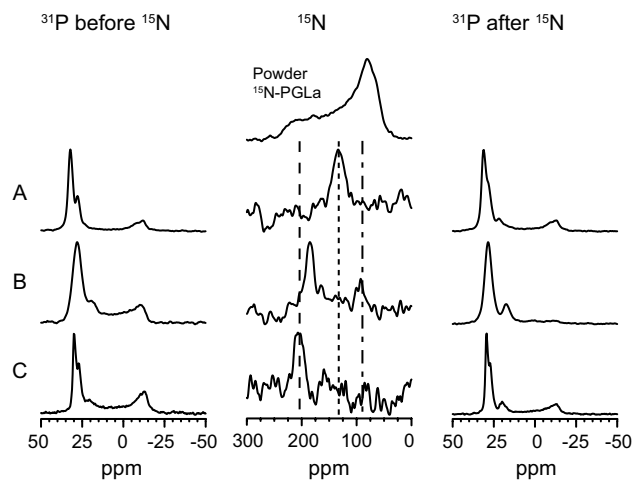


**Fig. 3**  $^{15}\text{N}$ -NMR of  $^{15}\text{N}$ -labeled PGLa in oriented lipid bilayers of DMPC/DMPG (3/1 molar ratio), in the absence and presence of unlabeled MAG2. The total *P/L* ratio was always 1/50. The powder spectrum of  $^{15}\text{N}$ -labeled PGLa (unoriented, dry peptide powder without lipids) is shown at the top of the middle column. The dashed line at 205 ppm corresponds to PGLa in the I-state, the dotted line at 130 ppm is characteristic of PGLa in the T-state, and the dash-dotted line represents the S-state. **a**  $^{15}\text{N}$ -PGLa; **b**  $^{15}\text{N}$ -PGLa + MAG2 (2/1); **c**  $^{15}\text{N}$ -PGLa + MAG2 (1/1). The  $^{31}\text{P}$ -NMR spectra before and after the  $^{15}\text{N}$ -NMR experiment show that all samples are well oriented. All NMR experiments were performed at  $35^\circ\text{C}$ , above the gel-to-liquid crystalline phase transition temperature of the lipids

a stable, long-lived complex. The total *P/L* ratio in these samples was 1/50, so in this 2/1 mixture the PGLa/MAG2/lipid ratio was 2/1/150, and the concentration of free PGLa was 1/150, whereas in Fig. 3a the concentration was 1/50. It is known that PGLa alone undergoes a concentration-dependent re-orientation from an S-state to the T-state (Strandberg et al. 2006; Tremouilhac et al. 2006a), which explains why the free PGLa signal is at slightly different positions in Fig. 3a and c.

If the inserted PGLa were to form a 1/1 complex with MAG2, in the 2/1 mixture we would then expect that the same number of PGLa molecules would be in the complex as there are in free form; however, the peak at 95 ppm was significantly smaller. Nonetheless, the signal intensities cannot be compared directly, because these are cross-polarization (CP) spectra. Therefore, the area under the peak depends not only on the number of spins but also on the CP efficiency in the two populations, which in turn depends on the orientation of the N–H bond vector with respect to the magnetic field (which changes as the peptide changes its orientation). The signal intensity also depends on the mobility of the peptides, which is higher for free surface-bound PGLa than for inserted PGLa in a complex with MAG2 (Glaser et al. 2005; Strandberg et al. 2006; Tremouilhac et al. 2006a). The optimal mixing time can also be different, which makes it difficult to obtain comparable

signals of the two peptides with dissimilar orientations/mobilities, and therefore does not allow the direct integration of the peaks. Even though it was not possible to quantitatively determine the PGLa/MAG2 ratio with the highest synergy from these NMR experiments, these data were fully compatible with the leakage assay results. Moreover, it is reasonable to assume that a 1/1 molar ratio of the peptides is also the best condition to study synergy in the NMR samples. Thus, for the remaining experiments in this study, we used 1/1 mixtures of PGLa and MAG2.

### Concentration dependence

#### Leakage

As seen above (Fig. 2), a 1/1 mixture of PGLa and MAG2 produced much more vesicle leakage than each peptide on its own, thus showing a strong and synergistic interaction between these two partners. The synergy was further investigated in POPC/POPG vesicles. The Hill coefficients were determined from the concentration-dependent leakage signals (Fig. 4) by fitting the initial rates to the Hill equation (Eq. 2). In other publications, the Hill coefficients from the leakage data have been evaluated by using partial dye release after a certain time (Das and Matile 2002; Talukdar et al. 2004). However, we rather analyzed and used the initial rate of leakage within the first 10 s for two reasons: (1) the leakage process is limited per se, because it cannot exceed 100 %, and the leakage data at later times will be affected by saturation effects; and (2) some of the leakage signals are curved and do not rise with a constant slope (cf. Fig. 4, MAG2 and PGLa/MAG2). Therefore, a reliable parameter of the pore formation process is better represented by the initial rate of vesicle leakage than by a distinct leakage value at a certain time point.

For each peptide and the mixture, two independent concentration series were measured. The initial leakage rates of both series were determined and plotted against the peptide concentration. The Hill coefficients were obtained by fitting the data to Eq. (2). The result is shown in Fig. 5, and the best-fit parameters are shown in Table 1.

For MAG2, a Hill coefficient ( $n$ ) of approximately 2 was found, whereas PGLa yielded  $n \approx 4$  and PGLa/MAG2 yielded  $n > 7$ . Thus, using Hill coefficients as a measure of cooperativity (Das and Matile 2002; Talukdar et al. 2004), we observed some cooperativity for MAG2, a stronger cooperativity for PGLa, and the most pronounced cooperativity for PGLa/MAG2. Given that  $K_H$ , representing the peptide concentration at which the half-maximal rate is observed, is a measure of the interaction strength, a larger  $K_H$  should indicate a weaker interaction. Hence, the following order of interaction strengths is obtained: MAG2/

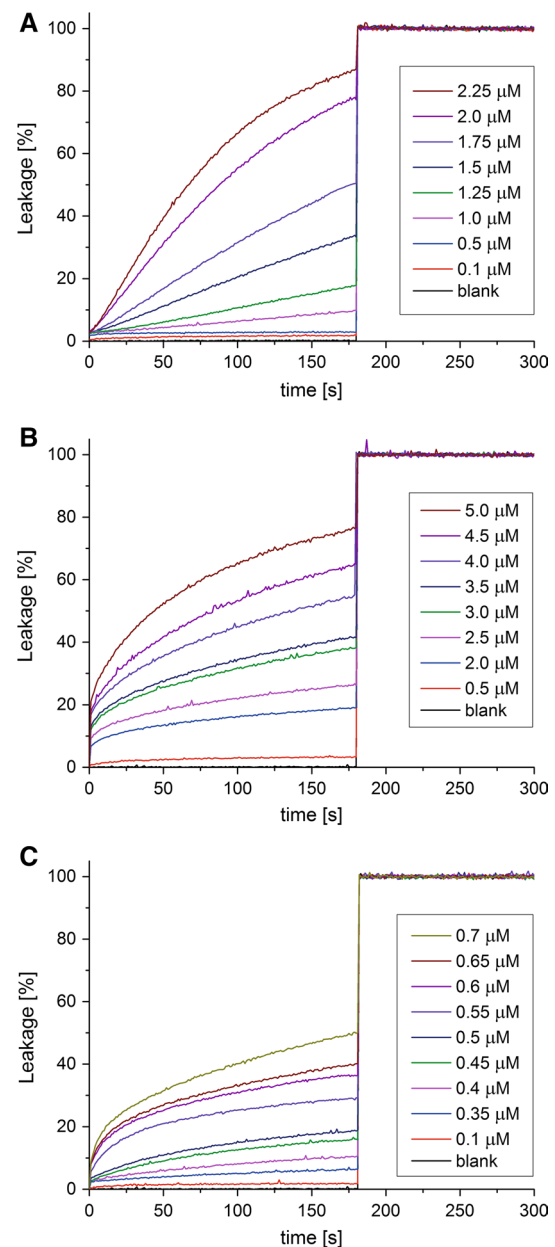


**Fig. 4** Examples of the time course of vesicle leakage at different peptide concentrations and a temperature of 30 °C. **a** PGLa; **b** MAG2; **c** PGLa/MAG2 1/1. The POPC/POPG (3/1) concentration was kept at 100  $\mu\text{M}$  and the amount of added peptide was varied, as shown in the *individual panels*. Note that different concentration ranges were used for each peptide system

MAG2 < PGLa/PGLa < PGLa/MAG2. In these experiments, the lipid concentration was kept fixed at 100  $\mu\text{M}$ , and the  $K_H$  values (peptide concentrations in  $\mu\text{M}$ ) were converted to the respective peptide-to-lipid molar ratios, at which half-maximum leakage is observed. This results in the series of  $P/L \approx 1/143$  for PGLa/MAG2, 1/36 for PGLa/PGLa, and 1/12 for MAG2/MAG2. These values will be discussed below.

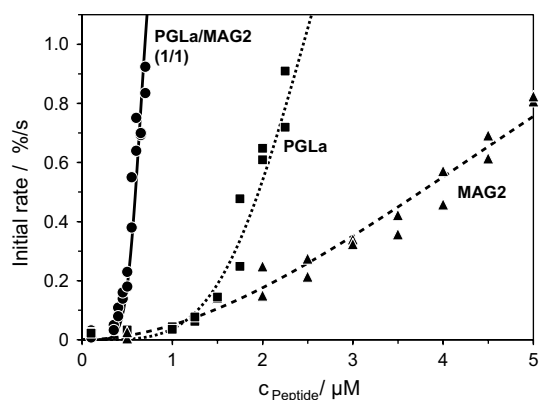


**Fig. 5** The initial rate of leakage plotted against the peptide concentration of PGLa (dotted line, filled squares), MAG2 (dashed line, filled triangles) or a 1:1 peptide mixture (solid line, filled circles). The curves are the best fits calculated from the Hill equation using the data analysis software Origin (OriginLab Corporation). The best-fit parameters are given in Table 1

**Table 1** Hill coefficient ( $n$ ), constant  $K_H$ , and maximum leakage rate ( $v_{max}$ ), determined from a fit of the leakage data at different peptide concentrations to the Hill equation (Eq. 2)

Peptide	$n$	$K_H$ [ $\mu\text{M}$ ]	$v_{max}$ [%/s]
PGLa	4.2 (0.7)	2.8 (0.2)	2.8 (0.5)
MAG2	1.9 (0.2)	8.0 (0.7)	2.6 (0.4)
PGLa/MAG2	7.4 (1.9)	0.7 (0.1)	1.8 (0.6)

Standard deviations are given in brackets

## $^{15}\text{N}$ -NMR

Because the results above showed that the PGLa–PGLa interactions are only slightly weaker than the PGLa–MAG2 interactions, we wondered whether there are any other, structural aspects that might contribute to the substantial synergistic enhancement of bilayer permeabilization. We thus performed  $^{15}\text{N}$ -NMR experiments to find out whether PGLa was able to undergo any full re-alignment into the transmembrane inserted state (i.e., the putative pore) in the absence of MAG2. Aiming for the highest possible  $P/L$  ratio, we were able to obtain well oriented samples up to  $P/L = 1/10$ . Even if the chemical shift of the PGLa peak is seen to change by about 20 ppm (from 133 ppm at  $P/L = 1/50$  to 153 ppm at  $P/L = 1/10$ ), the helix does not flip into the fully inserted state (which would give a peak at 205 ppm) that was found in the presence of MAG2 at an equivalent peptide-to-peptide-to-lipid molar ratio ( $P/P/L$ ) of 1/1/100 (Fig. 6). It can thus be concluded that PGLa alone never reached an inserted orientation in the liquid crystalline DMPC/DMPG bilayers, indicating that specific PGLa–MAG2 interactions are responsible for the full

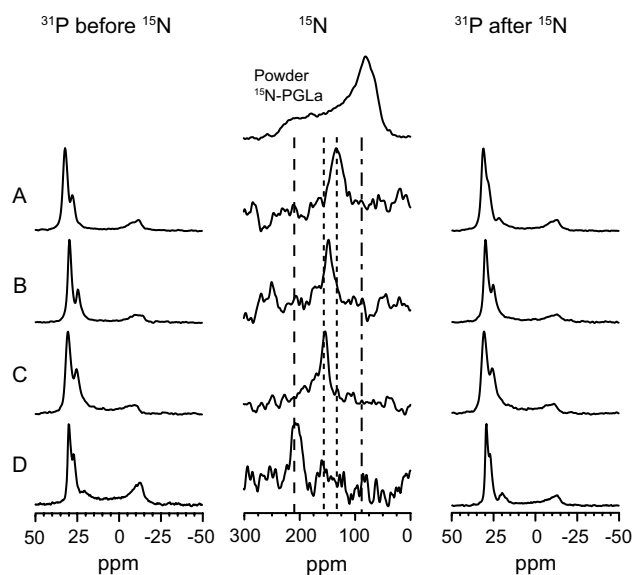


**Fig. 6**  $^{15}\text{N}$ -NMR and  $^{31}\text{P}$ -NMR spectra of  $^{15}\text{N}$ -PGLa at very high  $P/L$  ratios in DMPC/DMPG (3/1) bilayers, in the absence and presence of unlabeled MAG2. The dashed line at 205 ppm represents the inserted I-state, the dash-dotted line represents the S-state, and the range between the two dotted lines at 130 and 153 ppm is characteristic of a tilted T-state. (a)  $^{15}\text{N}$ -PGLa,  $P/L = 1/50$ ; (b)  $^{15}\text{N}$ -PGLa,  $P/L = 1/25$ ; (c)  $^{15}\text{N}$ -PGLa,  $P/L = 1/10$ ; (d)  $^{15}\text{N}$ -PGLa + MAG2 (1/1),  $P/L = 1/50$

insertion of PGLa under these conditions in the presence of MAG2.

Interestingly, previous  $^{15}\text{N}$ -NMR experiments have shown that in pure POPC bilayers and in POPC/POPG mixtures, PGLa remains always on the membrane surface in an S-state, even in the presence of MAG2 at  $P/P/L = 1/1/100$  (Salnikov and Bechinger 2011; Strandberg et al. 2013). This means that the PGLa–MAG2 interactions are not only specific but also lipid-dependent. Because PGLa alone can achieve an obliquely inserted T-state in DMPC or DMPC/DMPG but not in POPC or POPC/POPG (Strandberg et al. 2013), we speculate that the synergistic interaction can occur only when the PGLa helix (at least the C-terminus) is buried somewhat deeper in the membrane, which does not seem to occur in POPC. This behavior would again indicate a quite specific interaction between the peptides.

## $^{19}\text{F}$ -NMR

Using solid-state  $^{15}\text{N}$ -NMR, we have recently studied the structure and orientation of MAG2 in lipid bilayers, alone and in the presence of PGLa, to investigate how MAG2 responds as a function of concentration and lipid variation. We found that MAG2 alone lies essentially flat in the membrane, but together with PGLa it can achieve a slightly



tilted orientation (Strandberg et al. 2013). To investigate the PGLa-MAG2 interaction strength in a lipid bilayer, we now studied the orientation of MAG2 at lower concentrations, with and without PGLa. Because  $^{15}\text{N}$ - and  $^2\text{H}$ -NMR are quite insensitive methods and  $^2\text{H}$ -NMR also may exhibit background signals from lipids at low peptide concentrations (Grasnick et al. 2011), we used  $^{19}\text{F}$ -NMR as a more sensitive alternative. MAG2 was labeled at position Val17 or Gly18 with a single site-selective  $\text{CF}_3$ -Bpg reporter group. Previously, it had been shown that these mutations do not disturb the antimicrobial activity of MAG2, its synergistic effect with PGLa, or the secondary structure of the peptide (Strandberg et al. 2015). The  $^{19}\text{F}$ -NMR samples were prepared with 1/1 mixtures of PGLa/MAG2 at different  $P/P/L$  ratios, in order to determine the concentration at which the PGLa-MAG2 interaction starts to be observed. The  $^{31}\text{P}$ -NMR experiments showed that all of the samples were well oriented (Fig. S1).

Figure 7 shows the  $^{19}\text{F}$ -NMR spectra of MAG2- $^{19}\text{F}$ -V17 in oriented DMPC/DMPG (3/1) lipid bilayers. They were measured at two different macroscopic alignment angles of the oriented samples: with the membrane normal aligned parallel to the magnetic field ( $0^\circ$  tilt), or perpendicular to the membrane normal ( $90^\circ$  tilt). At  $0^\circ$  tilt, the samples yielded well-resolved splittings, which are analyzed below. At  $90^\circ$  tilt, the resolution was worse, but the signal was observed to shift to the other side of the isotropic position. The splittings were found to be scaled by a factor of approximately  $-1/2$ , and no powder pattern was observed. All these criteria indicate that MAG2 is engaged in rapid rotational diffusion around the membrane normal in all cases. Previous  $^{15}\text{N}$ -NMR studies have shown that at  $P/L = 1/50$ , MAG2 alone is in an S-state, whereas the orientation changes to a slightly inserted state in a 1/1 mixture with PGLa at  $P/P/L = 1/1/100$  (Strandberg et al. 2013). Here, we observed a clear triplet with a splitting of  $-4.3$  kHz at 1/50 (Fig. 7a). At a lower MAG2 concentration of 1/500, the splitting was the same as at 1/50, showing that the peptide orientation did not change. Obviously, MAG2 remained on the membrane surface as monomers at 1/50 and all lower concentrations (Fig. 7b). When PGLa was added to MAG2 in a 1/1 ratio at a  $P/P/L$  of 1/1/100, the splitting changed to  $-6.6$  kHz. There was only one splitting, indicating that there was only one population of peptides in the complex. At a low peptide concentration, the splitting of MAG2 in the presence of PGLa was the same as that without PGLa; in the 1/1/1000 sample, the splitting was the same as in the 1/500 sample (Fig. 7c). Thus, at low concentrations, the peptides were present as separate monomers, which were usually far from each other in the membrane and did not interact. At 1/1/600, the  $-4.3$ -kHz splitting was still present, but the larger  $-6.6$ -kHz splitting started to emerge (Fig. 7d), which then became dominant

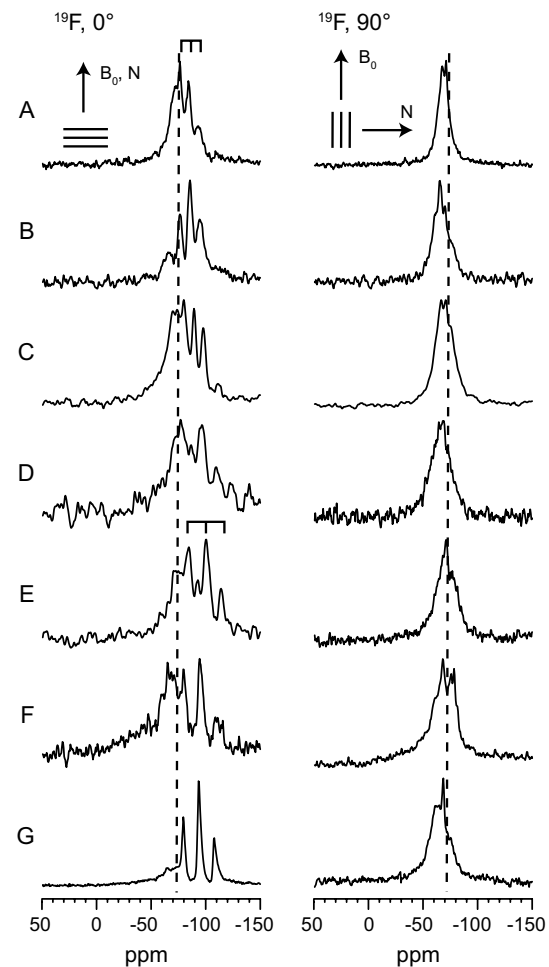


**Fig. 7**  $^{19}\text{F}$ -NMR spectra of MAG2- $^{19}\text{F}$ -V17 at different concentrations in oriented DMPC/DMPG (3/1) lipid bilayers, measured at a sample alignment of  $0^\circ$  and  $90^\circ$ , in the absence and presence of unlabeled PGLa. The dashed line indicates the isotropic chemical shift at  $-72$  ppm. (a)  $P/L = 1/50$ ; (b)  $P/L = 1/500$ ; (c) +PGLa,  $P/P/L = 1/1/1000$ ; (d) +PGLa,  $P/P/L = 1/1/600$ ; (e) +PGLa,  $P/P/L = 1/1/400$ ; (f) +PGLa,  $P/P/L = 1/1/200$ ; (g) +PGLa,  $P/P/L = 1/1/100$

at 1/1/400. The smaller splitting was no longer observed at 1/1/200 (Fig. 7e–g). All splittings are listed in Table S1. From these results, it appeared that the heterooligomeric assemblies start to form at a concentration between 1/1/1000 and 1/1/600, and at concentrations of 1/1/400 the heterooligomeric assemblies prevail.

The same experiments were also performed using MAG2- $^{19}\text{F}$ -G18, in order to obtain independent data for a different labeled position (with different geometry and splittings). These experiments also demonstrated a clear change from a splitting of 2 kHz in a 1/50 or 1/1/1000 sample, to a splitting of 13 kHz in a 1/1/100 sample. A superposition of the two splittings was observed at intermediate concentrations (Fig. S2). Thus, we observed the same effect of PGLa on both  $^{19}\text{F}$ -labeled MAG2 analogues, and

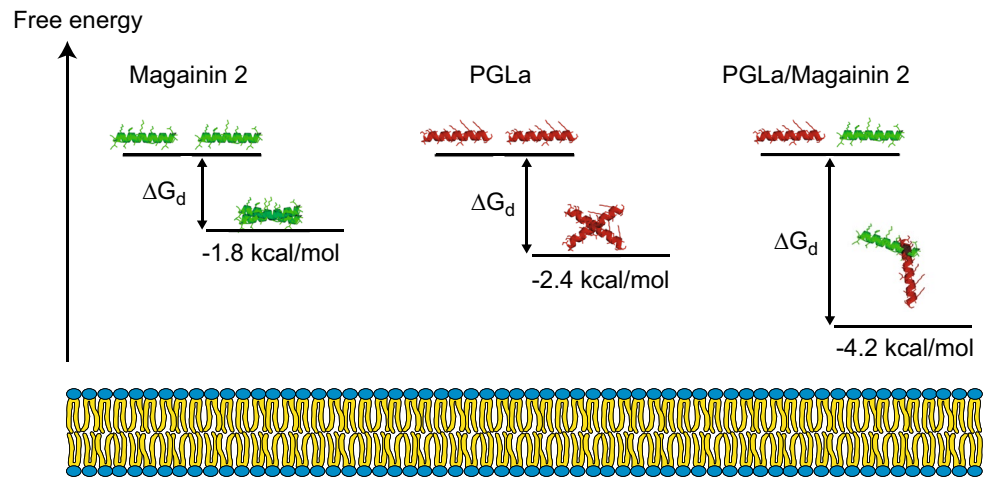


**Fig. 8** Free energy of dimerization of MAG2, PGLa, and PGLa/MAG2. Heterodimers are clearly more favorable than homodimers. The detailed structure of the heterodimer is unknown and therefore only schematically illustrated, but the membrane alignment of each

peptide in each state is drawn according to the present state of knowledge (Glaser et al. 2005; Strandberg et al. 2009, 2006, 2013; Tremouilhac et al. 2006a). Underneath, an oriented lipid bilayer is indicated as the frame of orientational reference, drawn to scale

the threshold for the interaction was approximately 1/1/600 in both cases. At 1/1/200, MAG2 preferentially formed heterodimers with PGLa. An interaction between MAG2 and PGLa in the membrane was not observed at very low peptide concentration, and thus was rather weak.

### Free energy calculations

To determine the interaction strength more quantitatively, the association constant or free energy of complex formation can be estimated from the biophysical data. In a previous study, Matsuzaki et al. have used a more advanced analysis allowing for any type of 1/1 complex, but they concluded that heterodimer formation could explain the data (Matsuzaki et al. 1998). Therefore, on the assumption that heterodimers are formed, we calculated the free energy of dimerization,  $\Delta G_d$ . The leakage activity is most likely explained by pore formation (Matsuzaki 1998; Matsuzaki et al. 1998, 1995a, 1995b), and such pores supposedly represent larger assemblies. Thus, dimerization would be the first, rate-determining step in leakage, which is then accompanied by the assembly of several heterodimers into a pore.

It is possible to use oriented circular dichroism (OCD) to estimate  $\Delta G_d$  for the homodimerization of PGLa and of MAG2 in membranes. For PGLa, the OCD spectra have been previously reported in DMPC at different  $P/L$  values, and a change of orientation from S-state to T-state has been observed with increasing peptide concentrations (Bürck et al. 2008). It is justified to assume that the S-state corresponds to monomers and the T-state to dimers, as previously proposed (Glaser et al. 2005; Tremouilhac et al.

2006a; Ulmschneider et al. 2012). We can thus estimate that half the peptides are in the form of monomers and half in dimers at  $P/L = 1/50$ , based on the previously reported concentration dependence of the OCD data (Bürck et al. 2008). This means that the peptide-to-lipid molar ratio for the monomers is  $[M] = 1/100$ , and  $[D] = 1/200$  for the dimers. By inserting these values into Eqs. (4) and (6), we found that  $\Delta G_d \approx -2.4$  kcal/mol for PGLa homodimerization. In a similar way, we used the previously published OCD data from magainin 1 in DMPC/DMPG (3/1) membranes (Ludtke et al. 1994). Based on these curves, we estimated that half of the peptides form dimers at  $P/L = 1/20$ , which leads to  $\Delta G_d \approx -1.8$  kcal/mol for magainin homodimerization. Using a fluorescence-based method, Matsuzaki et al. have previously found a similar value for MAG2,  $\Delta G_d = -2.1$  kcal/mol (Matsuzaki et al. 1998). The lower dimerization affinity of the magainin peptides compared to PGLa fits well with the Hill coefficients determined above. From the  $^{19}\text{F}$ -NMR spectra of MAG2 in DMPC/DMPG (3/1) in the presence of equimolar PGLa (Figs. 7 and S2), we estimated that there are approximately equal amounts of MAG2 present in monomers and in heterodimers at  $P/P/L = 1/1/500$ . This means  $[P] = [M] = 1/1000$  and  $[PM] = 1/1000$ , so we calculated  $\Delta G_d \approx -4.2$  kcal/mol from Eqs. (6) and (4) for PGLa-magainin heterodimerization. Using yet another method, Matsuzaki et al. have previously found a similar value,  $\Delta G_d = -3.6$  kcal/mol (Matsuzaki et al. 1998). An overview of the free energy results is shown in Fig. 8.

There is a significant difference in the free energy of dimerization of about 1.8 kcal/mol between the PGLa-PGLa homodimers and the PGLa-MAG2 heterodimers.

From the MAG2 point of view, the difference is even larger, approximately 2.4 kcal/mol. This means that heterodimer formation is clearly favored over homodimer formation for both MAG2 and PGLa, which is in good agreement with the Hill coefficients described above. This is also in agreement with the higher antimicrobial activity of PGLa over MAG2 and the even higher activity of PGLa/MAG2 in an equimolar mixture.

The total *P/L* ratio at which half of the peptides are present as monomers and the other half form dimers was found to be 1/250 (PGLa/MAG2), 1/50 (PGLa), and 1/20 (MAG2), as described above. We then compared these values with the *P/L* ratios at which the leakage rate was half the maximum: 1/143 (PGLa/MAG2), 1/36 (PGLa), and 1/12 (MAG2). In all three cases, the half maximum rate of leakage was observed at approximately 1.5 times the *P/L*, at which half of the peptides were in complexes. A stronger peptide interaction thus appears to be directly correlated with a higher leakage rate, most probably through the formation of a higher number of pores and/or longer-lived pores.

Compared to some other membrane protein dimers, the heterodimers of PGLa and MAG2 exhibit a rather weak interaction. For example, the well-known dimers formed by the transmembrane helix of glycophorin A have  $\Delta G_d \approx -7$  kcal/mol in  $C_8E_5$  detergent micelles (Fleming et al. 2004) or even  $-12$  kcal/mol in POPC vesicles (Hong et al. 2010). On the other hand,  $\Delta G_d \approx -3$  kcal/mol for the transmembrane domain of the FGF-receptor 3 in POPC vesicles (You et al. 2005) represents a value that is similar to the interaction strength calculated here for PGLa and MAG2.

## Conclusions

The synergistic interaction between PGLa and MAG2 increases their antimicrobial activity in vivo and vesicle leakage in vitro by a factor of more than 10, and here we have investigated this synergy with a range of complementary biophysical methods. Using a vesicle leakage assay, we observed the strongest synergy in a 1/1 mixture of PGLa/MAG2 in two different lipid compositions, suggesting that the synergy is probably caused by heterodimers or some other 1/1 complex. Higher synergy factors were observed in those vesicles that mimicked bacterial membranes. Our solid-state NMR data were compatible with the 1/1 complex hypothesis. The leakage experiments showed that PGLa-MAG2 interactions were stronger than PGLa-PGLa interactions, which were in turn stronger than MAG2-MAG2 interactions. Here, we quantified the interaction strength in the membrane by determining the Hill coefficients and free energy estimates. The Hill coefficient was

approximately 2 for MAG2-MAG2, 4 for PGLa-PGLa, and above 7 for PGLa-MAG2. The free energy of dimerization was estimated to be  $-1.8$  kcal/mol for MAG2,  $-2.4$  kcal/mol for PGLa, and  $-4.2$  kcal/mol for PGLa-MAG2 (Fig. 8). These values are similar to the free energy values that have been previously determined using other methods (Matsuzaki et al. 1998). The heterodimeric PGLa-MAG2 interaction in a membrane was to occur already at a *P/P/L* of 1/1/600 (according to  $^{19}\text{F}$ -NMR), whereas homodimers of PGLa-PGLa and MAG2-MAG2 were found to form only at much higher peptide-to-lipid ratios. This high heteromeric affinity is probably due to specific PGLa-MAG2 interactions. More studies are needed to better understand the molecular PGLa-MAG2 recognition on an atomistic scale.

**Acknowledgments** This work was supported financially by the Center for Functional Nanotechnology (CFN) (E1.2). We thank Andrea Eisele, Kerstin Scheubeck and Markus Schmitt for technical support.

## Compliance with ethical standards

**Conflicts of interest** The authors declare no conflict of interest.

## References

- Ammann C, Meier P, Merbach AE (1982) A simple multi-nuclear NMR thermometer. *J Magn Reson* 46:319–321
- Avanti Polar Lipids (2015) *E. coli* polar lipid extract. [http://www.avantilipids.com/index.php?option=com\\_content&view=article&id=409&Itemid=124&catnumber=100600](http://www.avantilipids.com/index.php?option=com_content&view=article&id=409&Itemid=124&catnumber=100600). Accessed 07 Dec 2015
- Bechinger B, Gierasch LM, Montal M, Zasloff M, Opella SJ (1996) Orientations of helical peptides in membrane bilayers by solid state NMR spectroscopy. *Solid State Nucl Magn Reson* 7:185–191
- Bennett AE, Rienstra CM, Auger M, Lakshmi KV, Griffin RG (1995) Heteronuclear decoupling in rotating solids. *J Chem Phys* 103:6951–6958
- Boman HG (1991) Antibacterial peptides: key components needed in immunity. *Cell* 65:205–207
- Boman HG (2003) Antibacterial peptides: basic facts and emerging concepts. *J Int Med* 254:197–215
- Brogden KA (2005) Antimicrobial peptides: pore formers or metabolic inhibitors in bacteria? *Nat Rev Microbiol* 3:238–250
- Bürck J, Roth S, Wadhvani P, Afonin S, Kanithasen N, Strandberg E, Ulrich AS (2008) Conformation and membrane orientation of amphiphilic helical peptides by oriented circular dichroism. *Biophys J* 95:3872–3881
- Carpino LA, Han GY (1972) 9-Fluorenylmethoxycarbonyl amino-protecting group. *J Org Chem* 37:3404–3409
- Chen L, Merzlyakov M, Cohen T, Shai Y, Hristova K (2009) Energetics of ErbB1 transmembrane domain dimerization in lipid bilayers. *Biophys J* 96:4622–4630
- Cujova S, Bednarova L, Slaninova J, Straka J, Cerovsky V (2014) Interaction of a novel antimicrobial peptide isolated from the venom of solitary bee *Colletes daviesanus* with phospholipid vesicles and *Escherichia coli* cells. *J Pept Sci* 20:885–895

- Das G, Matile S (2002) Transmembrane pores formed by synthetic *p*-octiphenyl  $\beta$ -barrels with internal carboxylate clusters: regulation of ion transport by pH and  $Mg^{2+}$ -complexed 8-aminonaphthalene-1,3,6-trisulfonate. *Proc Natl Acad Sci USA* 99:5183–5188
- Dempsey CE, Ueno S, Avison MB (2003) Enhanced membrane permeabilization and antibacterial activity of a disulfide-dimerized magainin analogue. *Biochemistry* 42:402–409
- Endreyi L, Fajsz C, Kwong FH (1975) Evaluation of Hill slopes and Hill coefficients when the saturation binding or velocity is not known. *Eur J Biochem* 51:317–328
- Fleming KG, Ren CC, Doura AK, Easley ME, Kobus FJ, Stanley AM (2004) Thermodynamics of glycoprotein A transmembrane helix dimerization in C14 betaine micelles. *Biophys Chem* 108:43–49
- Fung BM, Khitritin AK, Ermolaev K (2000) An improved broadband decoupling sequence for liquid crystals and solids. *J Magn Reson* 142:97–101
- Gesell J, Zasloff M, Opella SJ (1997) Two-dimensional  $^1H$  NMR experiments show that the 23-residue magainin antibiotic peptide is an  $\alpha$ -helix in dodecylphosphocholine micelles, sodium dodecylsulfate micelles, and trifluoroethanol/water solution. *J Biomol NMR* 9:127–135
- Glaser RW, Ulrich AS (2003) Susceptibility corrections in solid-state NMR experiments with oriented membrane samples. Part I: applications. *J Magn Reson* 164:104–114
- Glaser RW, Sachse C, Dürr UHN, Wadhvani P, Ulrich AS (2004) Orientation of the antimicrobial peptide PGLa in lipid membranes determined from  $^{19}F$ -NMR dipolar couplings of 4- $CF_3$ -phenylglycine labels. *J Magn Reson* 168:153–163
- Glaser RW, Sachse C, Dürr UHN, Afonin S, Wadhvani P, Strandberg E, Ulrich AS (2005) Concentration-dependent realignment of the antimicrobial peptide PGLa in lipid membranes observed by solid-state  $^{19}F$ -NMR. *Biophys J* 88:3392–3397
- Glattard E, Salnikov ES, Aisenbrey C, Bechinger B (2016) Investigations of the synergistic enhancement of antimicrobial activity in mixtures of magainin 2 and PGLa. *Biophys Chem* 210:35–44
- Grage SL, Strandberg E, Wadhvani P, Esteban-Martin S, Salgado J, Ulrich AS (2012) Comparative analysis of the orientation of transmembrane peptides using solid-state  $^2H$ - and  $^{15}N$ -NMR: mobility matters. *Eur Biophys J* 41:475–482
- Grasnick D, Sternberg U, Strandberg E, Wadhvani P, Ulrich AS (2011) Irregular structure of the HIV fusion peptide in membranes demonstrated by solid-state NMR and MD simulations. *Eur Biophys J* 40:529–543
- Grau-Campistany A, Strandberg E, Wadhvani P, Reichert J, Bürck J, Rabanal F, Ulrich AS (2015) Hydrophobic mismatch demonstrated for membranolytic peptides, and their use as molecular rulers to measure bilayer thickness in native cells. *Sci Rep* 5:9388
- Greenspan L (1977) Humidity fixed points of binary saturated aqueous solutions. *J Res Nat Bur Stand A* 81:89–96
- Hara T, Kodama H, Kondo M, Wakamatsu K, Takeda A, Tachi T, Matsuzaki K (2001a) Effects of peptide dimerization on pore formation: antiparallel disulfide-dimerized magainin 2 analogue. *Biopolymers* 58:437–446
- Hara T et al (2001b) Heterodimer formation between the antimicrobial peptides magainin 2 and PGLa in lipid bilayers: a cross-linking study. *Biochemistry* 40:12395–12399
- Hong H, Blois TM, Cao Z, Bowie JU (2010) Method to measure strong protein-protein interactions in lipid bilayers using a steric trap. *Proc Natl Acad Sci USA* 107:19802–19807
- Juretic D (1990) Antimicrobial peptides of the magainin family: membrane depolarization studies on *E. coli* and cytochrome oxidase liposomes. *Stud Biophys* 138:79–86
- Latal A, Degovics G, Eppard RF, Eppard RM, Lohner K (1997) Structural aspects of the interaction of peptidyl-glycylleucine-carboxamide, a highly potent antimicrobial peptide from frog skin, with lipids. *Eur J Biochem* 248:938–946
- Lee DK, Brender JR, Sciacca MF, Krishnamoorthy J, Yu C, Ramamoorthy A (2013) Lipid composition-dependent membrane fragmentation and pore-forming mechanisms of membrane disruption by pexiganan (MSI-78). *Biochemistry* 52:3254–3263
- Levitt MH, Suter D, Ernst RR (1986) Spin dynamics and thermodynamics in solid-state NMR cross polarization. *J Chem Phys* 84:4243–4255
- Ludtke SJ, He K, Wu YL, Huang HW (1994) Cooperative membrane insertion of magainin correlated with its cytolytic activity. *Biochim Biophys Acta* 1190:181–184
- Matsuzaki K (1998) Magainins as paradigm for the mode of action of pore forming polypeptides. *Biochim Biophys Acta* 1376:391–400
- Matsuzaki K, Harada M, Funakoshi S, Fujii N, Miyajima K (1991) Physicochemical determinants for the interactions of magainins 1 and 2 with acidic lipid bilayers. *Biochim Biophys Acta* 1063:162–170
- Matsuzaki K, Murase O, Tokuda H, Funakoshi S, Fujii N, Miyajima K (1994) Orientational and aggregational states of magainin 2 in phospholipid bilayers. *Biochemistry* 33:3342–3349
- Matsuzaki K, Murase O, Fujii N, Miyajima K (1995a) Translocation of a channel-forming antimicrobial peptide, magainin 2, across lipid bilayers by forming a pore. *Biochemistry* 34:6521–6526
- Matsuzaki K, Murase O, Miyajima K (1995b) Kinetics of pore formation by an antimicrobial peptide, magainin 2, in phospholipid bilayers. *Biochemistry* 34:12553–12559
- Matsuzaki K, Mitani Y, Akada KY, Murase O, Yoneyama S, Zasloff M, Miyajima K (1998) Mechanism of synergism between antimicrobial peptides magainin 2 and PGLa. *Biochemistry* 37:15144–15153
- Pinheiro da Silva F, Machado MC (2012) Antimicrobial peptides: clinical relevance and therapeutic implications. *Peptides* 36:308–314
- Porcelli F, Buck-Koehntop BA, Thenarasu S, Ramamoorthy A, Veglia G (2006) Structures of the dimeric and monomeric variants of magainin antimicrobial peptides (MSI-78 and MSI-594) in micelles and bilayers, determined by NMR spectroscopy. *Biochemistry* 45:5793–5799
- Raetz CRH (1978) Enzymology, genetics, and regulation of membrane phospholipid synthesis in *Escherichia coli*. *Microbiol Rev* 42:614–659
- Rance M, Byrd RA (1983) Obtaining high-fidelity spin-1/2 powder spectra in anisotropic media—phase-cycled Hahn echo spectroscopy. *J Magn Reson* 52:221–240
- Rex S (1996) Pore formation induced by the peptide melittin in different lipid vesicle membranes. *Biophys Chem* 58:75–85
- Ruden S, Hilpert K, Berditsch M, Wadhvani P, Ulrich AS (2009) Synergistic interaction between silver nanoparticles and membrane-permeabilizing antimicrobial peptides. *Antimicrob Agents Chemother* 53:3538–3540
- Salnikov ES, Bechinger B (2011) Lipid-controlled peptide topology and interactions in bilayers: structural insights into the synergistic enhancement of the antimicrobial activities of PGLa and magainin 2. *Biophys J* 100:1473–1480
- Soravia E, Martini G, Zasloff M (1988) Antimicrobial properties of peptides from *Xenopus* granular gland secretions. *FEBS Lett* 228:337–340
- Steinbrecher T et al (2012) Peptide-lipid interactions of the stress-response peptide TisB that induces bacterial persistence. *Biophys J* 103:1460–1469
- Strandberg E, Ulrich AS (2004) NMR methods for studying membrane-active antimicrobial peptides. *Concepts Magn Reson A* 23A:89–120

- Strandberg E, Ulrich AS (2014) Dynamic structure analysis of peptides in membranes by solid-state NMR. In: Separovic F, Naito A (eds) *Advances in biological solid-state NMR: proteins and membrane-active peptides*. Royal Society of Chemistry, London, pp 304–319
- Strandberg E, Ulrich AS (2015) AMPs and OMPs: is the folding and bilayer insertion of  $\beta$ -stranded outer membrane proteins governed by the same biophysical principles as for  $\alpha$ -helical antimicrobial peptides? *Biochim Biophys Acta* 1848:1944–1954
- Strandberg E, Wadhvani P, Tremouilhac P, Dürr UHN, Ulrich AS (2006) Solid-state NMR analysis of the PGLa peptide orientation in DMPC bilayers: structural fidelity of  $^2\text{H}$ -labels versus high sensitivity of  $^{19}\text{F}$ -NMR. *Biophys J* 90:1676–1686
- Strandberg E, Tremouilhac P, Wadhvani P, Ulrich AS (2009) Synergistic transmembrane insertion of the heterodimeric PGLa/magainin 2 complex studied by solid-state NMR. *Biochim Biophys Acta* 1788:1667–1679
- Strandberg E, Tiltak D, Ehni S, Wadhvani P, Ulrich AS (2012) Lipid shape is a key factor for membrane interactions of amphipathic helical peptides. *Biochim Biophys Acta* 1818:1764–1776
- Strandberg E, Zerweck J, Wadhvani P, Ulrich AS (2013) Synergistic insertion of antimicrobial magainin-family peptides in membranes depends on the lipid spontaneous curvature. *Biophys J* 104:L9–11
- Strandberg E et al (2015) Influence of hydrophobic residues on the activity of the antimicrobial peptide magainin 2 and its synergy with PGLa. *J Pept Sci* 21:436–445
- Talukdar P, Sakai N, Sorde N, Gerard D, Cardona VM, Matile S (2004) Outer surface modification of synthetic multifunctional pores. *Bioorg Med Chem* 12:1325–1336
- Tremouilhac P, Strandberg E, Wadhvani P, Ulrich AS (2006a) Conditions affecting the re-alignment of the antimicrobial peptide PGLa in membranes as monitored by solid state  $^2\text{H}$ -NMR. *Biochim Biophys Acta* 1758:1330–1342
- Tremouilhac P, Strandberg E, Wadhvani P, Ulrich AS (2006b) Synergistic transmembrane alignment of the antimicrobial heterodimer PGLa/magainin. *J Biol Chem* 281:32089–32094
- Ulmschneider JP, Smith JC, Ulmschneider MB, Ulrich AS, Strandberg E (2012) Reorientation and dimerization of the membrane-bound antimicrobial peptide PGLa from microsecond all-atom MD simulations. *Biophys J* 103:472–482
- Ulrich AS (2005) Solid state  $^{19}\text{F}$ -NMR methods for studying biomembranes. *Progr Nucl Magn Reson Spect* 46:1–21
- Ulrich AS et al (2006) Solid-state  $^{19}\text{F}$ -nuclear magnetic resonance analysis of membrane-active peptides. In: Ramamoorthy A (ed) *NMR spectroscopy of biological solids*. CRC Press, Boca Raton, pp 215–236
- Vaz Gomes A, De Waal A, Berden JA, Westerhoff HV (1993) Electric potentiation, cooperativity, and synergism of magainin peptides in protein-free liposomes. *Biochemistry* 32:5365–5372
- Wadhvani P, Bürck J, Strandberg E, Mink C, Afonin S, Ulrich AS (2008) Using a sterically restrictive amino acid as a  $^{19}\text{F}$ -NMR label to monitor and control peptide aggregation in membranes. *J Am Chem Soc* 130:16515–16517
- Wadhvani P, Strandberg E, Heidenreich N, Bürck J, Fanghänel S, Ulrich AS (2012) Self-assembly of flexible  $\beta$ -strands into immobile amyloid-like  $\beta$ -sheets in membranes as revealed by solid-state  $^{19}\text{F}$ -NMR. *J Am Chem Soc* 134:6512–6515
- Wadhvani P, Strandberg E, van den Berg J, Mink C, Bürck J, Cirillo R, Ulrich AS (2014) Dynamical structure of the short multifunctional peptide BP100 in membranes. *Biochim Biophys Acta* 1838:940–949
- Wadhvani P et al. (2007) Using fluorinated amino acids for structure analysis of membrane-active peptides by solid-state  $^{19}\text{F}$ -NMR. In: Soloshonok VA, Mikami K, Yamazaki T, Welch JT, Honek JF (eds) *Current Fluoroorganic Chemistry: New Synthetic Directions, Technologies, Materials, and Biological Applications*. ACS Symposium Series 949. American Chemical Society, Washington, DC, pp 431–446
- Wakamatsu K, Takeda A, Tachi T, Matsuzaki K (2002) Dimer structure of magainin 2 bound to phospholipid vesicles. *Biopolymers* 64:314–327
- Walther TH, Grage SL, Roth N, Ulrich AS (2010) Membrane alignment of the pore-forming component TatA<sub>4</sub> of the twin-arginine translocase from *Bacillus subtilis* resolved by solid-state NMR spectroscopy. *J Am Chem Soc* 132:15945–15956
- Wang Y, Zhao T, Wei D, Strandberg E, Ulrich AS, Ulmschneider JP (2014) How reliable are molecular dynamics simulations of membrane active antimicrobial peptides? *Biochim Biophys Acta* 1838:2280–2288
- Westerhoff HV et al (1995) Functional synergism of the magainins PGLa and magainin-2 in *Escherichia coli*, tumor-cells and liposomes. *Eur J Biochem* 228:257–264
- Williams RW, Starman R, Taylor KM, Gable K, Beeler T, Zasloff M, Covell D (1990) Raman spectroscopy of synthetic antimicrobial frog peptides magainin 2a and PGLa. *Biochemistry* 29:4490–4496
- You M, Li E, Wimley WC, Hristova K (2005) Förster resonance energy transfer in liposomes: measurements of transmembrane helix dimerization in the native bilayer environment. *Anal Biochem* 340:154–164
- Zasloff M (1987) Magainins, a class of antimicrobial peptides from *Xenopus* skin: isolation, characterization of two active forms, and partial cDNA sequence of a precursor. *Proc Natl Acad Sci USA* 84:5449–5453
- Zhang S, Wu XL, Mehring M (1990) Elimination of ringing effects in multiple-pulse sequences. *Chem Phys Lett* 173:481–484